Macromolecular Materials and Engineering
Open Access
www.mame-journal.de

Fabrication of Multifunctional Composite Nanofibers by Green Electrospinning

Edurne González, Aitor Barquero, Maria Paulis, and Jose Ramon Leiza*

The present work takes advantage of green electrospinning to create novel composite multifunctional nanofibers (NFs) bearing inorganic nanoparticles (NPs), more specifically quantum dots (QDs), cerium oxide nanoparticles (CeO_2 NPs) and iron oxide nanoparticles (Fe_3O_4 NPs). This is achieved by first encapsulating the desired inorganic NPs into polymer particles by the use of miniemulsion polymerization, and second, spinning the hybrid polymer particles using polyvinyl alcohol (PVA) as template polymer. It is proved that using green electrospinning, it is not only possible to ensure an excellent distribution and encapsulation of the inorganic NPs along the NFs, but also allows to control and change the concentration, size, and type of the inorganic NPs without altering the NFs size, a fact that is not possible by conventional solution electrospinning. As proof of concept, NFs with up to three different types of inorganic NPs have been created in a single electrospinning step, but this technology allows to incorporate as much inorganic NPs as desired without altering the NFs morphology and ensuring a good distribution and encapsulation of the NPs. This paper demonstrates that green electrospinning is a powerful and attractive technology to create multifunctional NFs that are promising materials for sensing and biomedical applications.

1. Introduction

Electrospun polymer nanofiber mats are materials with a porous structure and a huge area-to-volume ratio. These properties make them useful for a broad range of applications such as textiles, filters, tissue engineering, drug delivery, wound healing, sensors, environmental remediation, and catalysis, among others.[1–5] Polymeric nanofibers (NFs) are usually created by solution electrospinning as it is a simple and cheap technology that allows to obtain NFs with diameters ranging from 10 nm to 1 µm. However, solution electrospinning presents some limitations for industrial applications, such as the need to use toxic, flammable organic solvents (in most cases), and low polymer concentrations. Solutions of high polymer concentrations cannot be spun due to their high viscosity, severely limiting the production rate. Suspension electrospinning, also named green electrospinning, is a novel technology that has emerged in the last years as a smart alternative to overcome the limitations of solution electrospinning. Green electrospinning consists of electrospinning an aqueous polymer (nano)particle dispersion (a latex) with the help of a polymer template (a water soluble polymer). Using this technology, hydrophobic polymers can be spun at higher concentrations than the ones used in solution electrospinning, using water as an electrospinning medium.[6–8]

The first paper on green electrospinning was published by Greiner and coworkers in 2007.[9] Since then, different works have been published using different template/particle ratios,[9–12] particles of different sizes,[9,10,13] T_g values,[13] surface functional groups,[14] or crosslinking densities.[15,16] However, there are very few works in the literature that have thoroughly studied and understood the influence of the initial dispersion composition and properties on the final fiber morphology. To this end, in our previous work,[8] we performed a systematic study that investigated the effect of the template polymer molar mass, the total solids content of the dispersion, the particle/template ratio, the surface chemistry, and the particle size distribution in a single work. We demonstrated that all these parameters affect the viscosity of the initial electrospinning dispersion and therefore, they have a strong influence on the final fiber morphology. The present work gives one step forward and ought to take advantage of green electrospinning to create novel multifunctional composite NFs bearing inorganic nanoparticles (NPs). For this work, quantum dots (QDs), cerium oxide nanoparticles (CeO_2 NPs), and iron oxide nanoparticles (Fe_3O_4 NPs) have been selected, as they are interesting materials for sensing, energy and biomedical applications.[17–22] NFs containing QDs or CeO_2 NPs have been prepared before, but they have been usually obtained by solution electrospinning.[23–31] To do so, the inorganic NPs have to be dispersed in the polymer solution that will be spun later. Therefore, compatibility between the inorganic NPs and the polymer/solvent system is of utmost importance, and feasible polymer/NPs combinations are often limited. Hydrophilic NPs must be used when water-soluble

E. González, A. Barquero, M. Paulis, J. R. Leiza
POLYMAT and Kimika Aplikatua Saila, Kimika Fakultatea, University of the Basque Country UPV/EHU, Joxe Mari Korta Zentroa
Tolosa Hiribidea 72, Donostia-San Sebastián 20018, Spain
E-mail: edurne.gonzlaezg@ehu.eus

The ORCID identification number(s) for the author(s) of this article can be found under https://doi.org/10.1002/mame.202300011

DOI: 10.1002/mame.202300011

Table 1. Properties of used latexes in terms of composition, solids content (s.c.), polymer particle diameter (dp) and type and amount of encapsulated inorganic NP.

Name of the latex	(co)polymer	s.c. [%]	dp [nm][a)]	Encapsulated inorganic NP	Amount of inorganic NPs [wbm %][b)]
L_QDs	PS/PMMA Core/shell	13	147 ± 1	CdSe/ZnS core/shell QDs	0.42
L_Fe_3O_4	PS	20	147 ± 2	Fe_3O_4	5
L_CeO_2_1%	P(MMA/BA /AA)	50	174 ± 1	CeO_2	1
L_CeO_2_5%	P(MMA/BA /AA)	50	183 ± 1	CeO_2	5
L_Blank	P(MMA/BA /AA)	50	139 ± 3	-	-

[a)]Z-average value obtained by DLS. The reported number is the average of three different measurements and the error represents the standard deviation of the different measurements. [b)]weight based on monomers (wbm)

polymers are desired to be spun,[23,24,27,28] whereas hydrophobic ones have to be used to spin hydrophobic polymers.[25,29–32] Although a good distribution of the QDs in the final NFs was observed in some cases,[23,26] when using CeO_2 NPs, non-uniform aggregates of the NPs along the NFs were obtained.[27,31,33] Additionally, the size of the final NFs was affected by the presence of the inorganic NPs, as the conductivity and viscosity of the electrospinning solution were increased by the addition of the inorganic NPs.[24,25,30,33] Other methods such as layer-by-layer deposition onto the NFs surface[14,20,34–37] or co-axial electrospinning[38,39] have also been used to create NFs containing inorganic NPs, but these last two methods are more complex or require several synthesis steps.

In the present article, polymeric NFs bearing QDs and CeO_2 NPs have been fabricated by green electrospinning. We demonstrate that green electrospinning is a promising and simple enough technique to obtain organic-inorganic nanocomposite NFs in a single electrospinning step without the use of any organic solvent. To do so, we first synthesized polymer particles bearing encapsulated QDs, CeO_2 NPs, or Fe_3O_4 NPs and then we spun these latexes using polyvinyl alcohol (PVA) as template polymer. To the best of our knowledge, there is only one article in the literature that has spun polymer particles containing inorganic NPs.[40] This work was performed in our group by De San Luis et al.[40] They synthesized core-shell crosslinked polystyrene/polymethyl methacrylate polymer particles containing QDs (QDs/PS/PMMA) and spun them using PVA or poly(ethylene oxide) (PEO) as a template polymer. By measuring the electric properties of the hybrid NFs, they demonstrated that the NFs had VOC sensing capacity. However, in that work, the authors did not pay any special attention to the morphology of the obtained NFs or the distribution and size of the inorganic NPs along the NFs. In this work, we demonstrate that the use of green electrospinning not only guarantees a good distribution of the inorganic NPs along the NFs, but also allows controlling the size and concentration of the inorganic NPs without altering the NFs diameter. We have also been able to synthesize NFs with up to three different types of inorganic NPs for the first time.

2. Experimental Section

2.1. Materials

Mowiol 25–88 polyvinyl alcohol (PVA) polymer (Mw: 92.6 kDa and a hydrolysis degree of 88%) was purchased from Kuraray to be used as a template polymer. A latex made of poly(methyl methacrylate-co-butyl acrylate-co-acrylic acid) (P(MMA/BA/AA)) (without any inorganic NPs) was used as blank latex. Additionally, four different latexes containing inorganic NPs were synthesized; a crosslinked core/shell polystyrene/poly(methyl methacrylate) (P(S/MMA)) latex containing CdSe/ZnS core/shell QDs, a polystyrene (PS) latex containing iron oxide (Fe_3O_4) NPs, and two different P(MMA/BA/AA) latexes containing 1 and 5 wbm % of CeO_2 NPs. **Table 1** summarizes the properties of the different latexes used in this work, their synthesis procedure is explained in section S.1 of the Supporting Information.

Table 2. Composition of the electrospinning blends prepared using different ratios between L_CeO_2_1% or L_CeO_2_5% and L_Blank.

Name	L_CeO_2_1% [g]	L_CeO_2_5% [g]	L_Blank [g]	PVA solution [g][a)]	CeO_2 [wbp %][b)]
B_CeO_2_1%_Low	0.60	0	1.90	9.25	0.15
B_CeO_2_1%_High	1.20	0	1.30	9.25	0.30
B_CeO2_5%_Low	0	0.120	2.38	9.25	0.15
B_CeO2_5%_High	0	0.240	2.26	9.25	0.30

[a)] PVA solution was 8.1 wt.% in water [b)] Weight based on the total polymer (particles+PVA) (wbp %) [c)] s.c. of the blends was 17 wt.% and the particle/PVA ratio was 62/38 wt.%/wt.% in all the cases

2.2. Preparation of Electrospinning Blends

The electrospinning blends were prepared in two steps; first, different latexes were mixed together and later this mixture was added to a PVA solution dropwise under magnetic stirring to obtain the electrospinning blend.

Two blend series were prepared. The first one (**Table 2**) was prepared with the objective to obtain NFs with different numbers and sizes of inorganic NPs , using the CeO_2 NPs as an example. To do so, CeO_2 NPs containing latexes (L_CeO_2_1% and L_CeO_2_5%) were mixed with the blank latex (L_Blank) and then blended with PVA. The number of CeO_2 NPs in the NFs was controlled with the ratio between the CeO_2-containing latex and the blank latex. The size of the CeO_2 NPs, on the other hand, was controlled by the amount of CeO_2 NPs that was encapsulated inside the hybrid polymer particles.[41,42] The polymer particles/PVA ratio was 62/38 wt.%/wt.% in all the blends and the total solids content (s.c.), that is, the concentration of the total polymer (polymer particles plus PVA) was 17 wt.%. All the blends were stable.

Table 3. Composition of electrospinning blends prepared using latexes with different types of inorganic NP.

Name	L_QD [g]	L_CeO_2_5% [g]	L_Blank [g]	L_Fe_3O_4 [g]	PVA solution [g][a)]	QD [wbp %][b)]	CeO_2 [wbp %][b)]
B_QDs	0.853	-	4.147	-	16.65	0.0124	-
B_QDs_CeO_2_1:1	0.853	0.018	4.129	-	16.65	0.0124	0.0124
B_QDs_CeO_2_1:2	0.853	0.037	4.111	-	16.65	0.0124	0.0249
B_QDs_CeO_2_Fe_3O_4	1.787	0.041	3.044	0.128	16.65	0.028	0.0298

[a)] PVA solution was 9 wt.% [b)] Weight based on the total polymer (particles+PVA) (wbp %) [c)] s.c. of the blends was 17 wt.% and particle/PVA ratio was 59/41 wt.%/wt.% in all the cases

The second blend series (**Table 3**) was prepared with the objective to obtain hybrid NFs containing different types and amounts of inorganic NPs. To do so, the latex containing QDs (L_QDs) was mixed with the one containing 5 wbm % of CeO_2 (L_CeO_2_5%), the latex containing Fe_3O_4 (L_Fe_3O_4) and the blank latex (L_Blank). This mixture was later added to the PVA solution. The polymer particles/PVA ratio was 59/41 wt.%/wt.% and the s.c. 17 wt.% in all the blends.

2.3. Electrospinning Experiments

Electrospinning experiments were performed using the vertical setup of SpinBox (Bioinicia). Randomly oriented nanofibers were obtained by applying a voltage of 15 kV, a flow rate of 0.25 mL h^{-1} and a tip-to-collector distance of 15 cm. The temperature and relative humidity (R.H.) of the electrospinning chamber were 23 ± 1 °C and 46 ± 2%, respectively.

2.4. Nanofiber Characterization

Polymer particle z-average diameter (dp) was measured by dynamic light scattering (Zetasizer Nano Z, Malvern Instruments, Malvern, UK). Nanofiber morphology was analyzed by scanning electron microscopy (SEM) in a Hitachi TM3030 Scanning Electron Microscope (Monocomp, Madrid, Spain). ImageJ™ open source software (National Institutes of Health, Bethesda, MD, USA) was used on the SEM images to measure the mean average fiber diameter. Fifty measurements were made for each sample from three separate images. Fluorescence spectroscopy measurements of the NFs mats were performed using an Epoch 2 Microplate Spectrophotometer (BioTek). NFs mats were cut using a paper hole puncher and placed on the microplate. Fluorescence emission spectra of the samples were monitored over the spectral window from 500 to 700 nm with a step size of 2 nm. The excitation wavelength was 400 nm. Transmission electron microscopy (TEM) experiments were performed on a Talos F200i field emission gun instrument equipped with a Bruker X-Flash100 XEDS spectrometer. Elemental maps were performed by XEDS in the STEM mode under a high annular dark field (HAADF) detector for Z contrast imaging in STEM conditions (camera length of 200 mm) using a pixel size of 2 nm, a dwell time of 900 s, and an image size of 512 × 512 pixels. Moreover, EDX microanalyses were carried out using a probe current of 250 pA and semiconvergence angle of 8.5 mrad.

3. Results and Discussion

3.1. Nanofibers with Different Size and Concentrations of CeO_2 Nanoparticles

First of all, three different acrylic latexes were synthesized and characterized. L_Blank was a P(MMA/BA/AA) copolymer latex and L_CeO_2_1% and L_CeO_2_5% were also P(MMA/BA /AA) copolymer latexes but containing 1 wbm % and 5 wbm % of CeO_2 NPs, respectively. **Figure 1** shows the TEM micrographs of latexes L_CeO_2_1% and L_CeO_2_5%. As observed by Aguirre and co-workers,[41,42] the encapsulated CeO_2 NPs (originally with a diameter of 12 nm) formed NPs aggregates inside the polymer particles and the size of these aggregates increased as the amount of encapsulated CeO_2 NPs was increased. It is also remarkable that each polymer particle contained a single CeO_2 NPs aggregate. The CeO_2 NPs aggregates in latex L_CeO_2_1% had an average diameter of 23 ± 7 nm whereas the ones in L_CeO_2_5% had an average diameter of 40 ± 9 nm.

With the objective to obtain hybrid NFs with CeO_2 NPs of different sizes and concentrations, electrospinning dispersions were prepared by mixing the latexes L_CeO_2_1% or L_CeO_2_5% with the blank latex (L_Blank) and blending it with PVA (see Table 2). PVA was used as a template polymer. The template polymer is necessary to form entanglements during the fiber formation and acts as a binder between the polymer particles.[8] All the dispersions had a s.c. of 17 wt.% and a polymer particles/PVA ratio of 62/38 wt.%/wt.%. In our previous work, we found that this particle/PVA ratio and s.c. were adequate to form continuous good quality fibers.[8] Changing the ratio between the latex containing CeO_2 NPs (L_CeO_2_1% or L_CeO_2_5%) and the blank latex (L_Blank) NFs with CeO_2 NPs concentrations of 0.15 wbm % (B_CeO_2_1%_Low and B_CeO_2_5%_Low) and 0.3 wbp % (B_CeO_2_1%_High and B_CeO_2_5%_High) were obtained. **Figure 2** shows the TEM and HAADF STEM micrographs of the obtained NFs. SEM images are shown in section S.2 of Supporting Information. Location of each CeO_2 NP is indicated by a pink arrow.

Two important conclusions can be clearly reached from Figure 2. The first one is that, as expected, the higher the ratio of the latex containing CeO_2 NPs in the initial electrospinning dispersion, the higher the concentration of CeO_2 NPs in the final fiber (there are more CeO_2 NPs per NF square area). The second conclusion is that a very good distribution of CeO_2 NPs was obtained in all the cases, and not only that, the size of the CeO_2 NPs did not change from the initial polymer particles to the final NFs. That is, CeO_2 NPs in the initial polymer particles

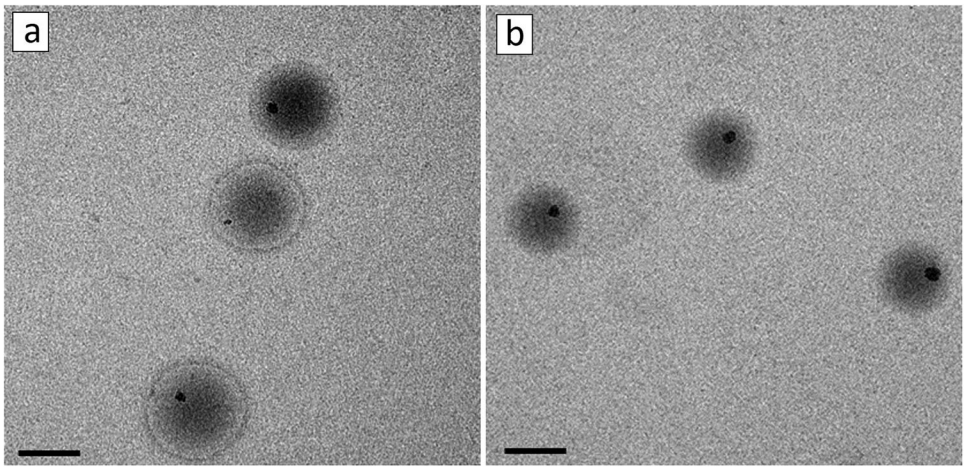

Figure 1. TEM micrograph of Latexes L_CeO_2_1% a) and L_CeO_2_5% b). Scale bar: 200 nm.

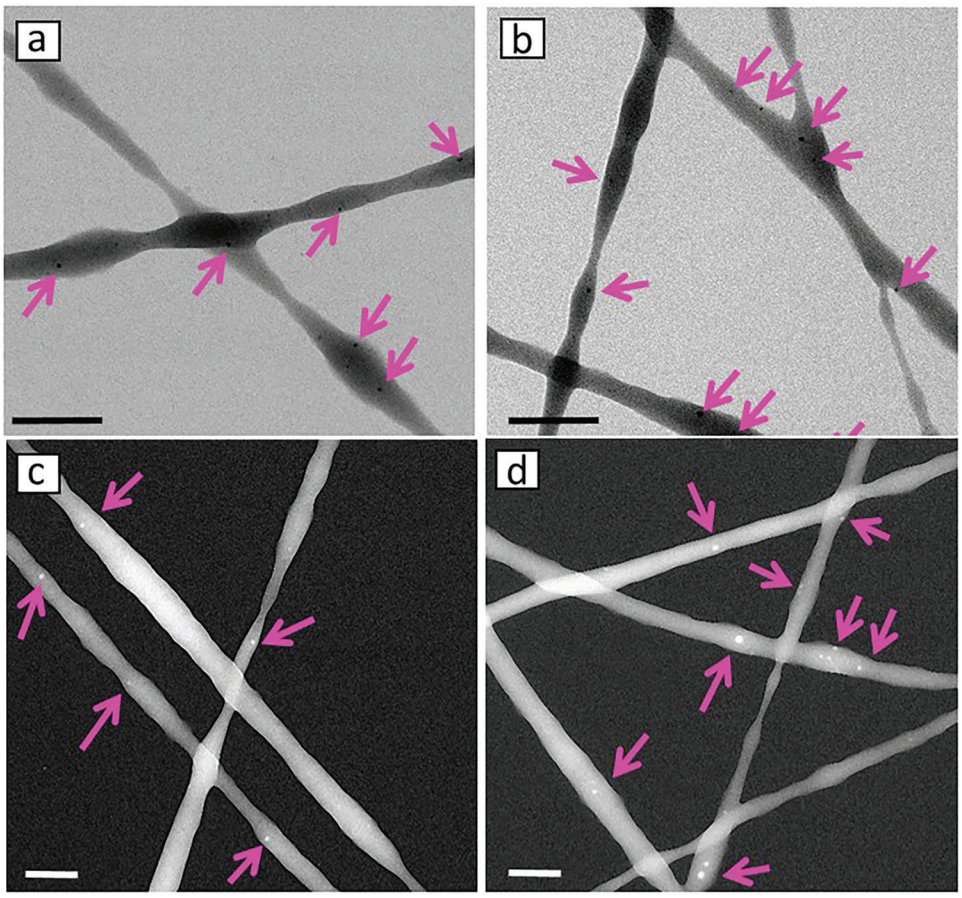

Figure 2. TEM ((a) and (b)) and HAADF STEM ((c) and (d)) micrographs of NFs obtained from the electrospinning dispersions B_CeO_2_1%_Low a), B_CeO_2_1%_High b), B_CeO_2_5%_Low c) and B_CeO_2_5%_High d). Scale bar: 500 nm.

did not suffer any aggregation during the fiber formation. This was confirmed by measuring the average CeO_2 NPs sizes in the NFs and comparing them with the values in the initial hybrid polymer particles. **Figure 3**(a) presents the average CeO_2 NPs sizes for the initial latex particles and the NFs containing 0.15 wbp % (B_CeO_2_1%_Low and B_CeO_2_5%_Low) and 0.3 wbp % (B_CeO_2_1%_High and B_CeO_2_5%_High) of CeO_2. Figure 3(a) clearly demonstrates that by controlling the amount of CeO_2 NPs that is encapsulated inside the polymer particles, it is possible to control the size of the CeO_2 NPs in the final fiber

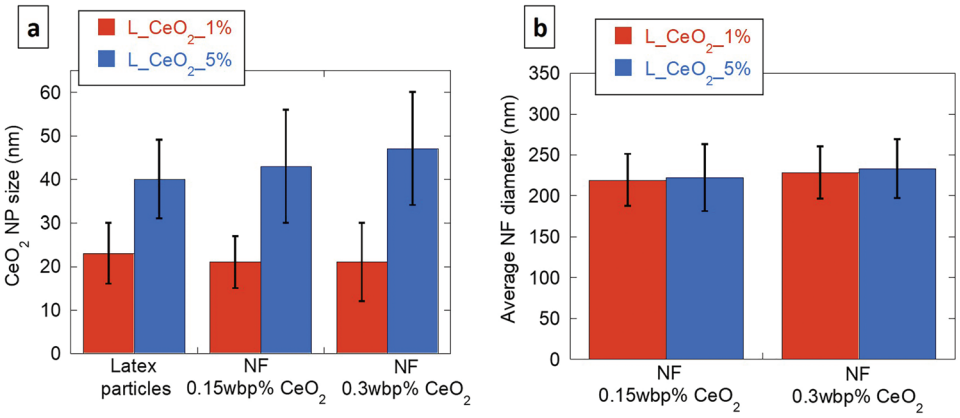

Figure 3. a) Average CeO_2 NPs size in the initial latexe particles and the final NFs containing 0.15 wbp % and 0.3 wbp % of CeO_2. b) Average diameter of the NFs containing 0.15 wbp % and 0.3 wbp % of CeO_2 NPs. NFs containing 0.15 wbp % of CeO_2 are the ones coming from B_CeO_2_1%_Low and B_CeO_2_5%_Low. NFs containing 0.30 wbp % of CeO_2 are the ones coming from B_CeO_2_1%_High and B_CeO_2_5%_High.

as these NPs do not suffer further aggregation during the fiber formation.

Additionally, the average fiber diameter of the four NFs samples was measured from the SEM images (shown in section S.2 in the Supporting Information). As it can be observed in Figure 3(b), all the NFs have a very similar average diameter (≈220 nm). These results are very interesting, since they probe that using green electrospinning it is possible to obtain NFs with different amounts and sizes of inorganic NPs keeping constant the fiber diameter. This cannot be achieved by conventional solution electrospinning. If organic-inorganic hybrid NFs are sought by solution electrospinning, the only way to do it is by dispersing the inorganic NPs in the initial polymer solution. After the electrospinning process, the inorganic NPs may suffer some aggregation, and therefore it is very difficult to control the size of these aggregates in the final NF.[27,31,33] Furthermore, the size of the NFs will be affected by the amount of inorganic NPs, since their presence alters the viscosity and conductivity of the electrospinning solution.[30,33,43,44] On the contrary, using green electrospinning it is possible to control the size of the inorganic NPs aggregates just by controlling the amount of NPs that it is encapsulated in the initial latex particles. Additionally, by controlling the number of hybrid polymer particles in the electrospinning blend, it is also possible to control the amount of inorganic NPs aggregates in the final fiber. Finally, the size of the NFs is not affected by the size and amount of inorganic NPs , since in green electrospinning the size of final NFs depends on the size of the polymer particles and the particle/PVA ratio.[8]

3.2. Fluorescents Nanofibers Containing QDs

As it has been done with the CeO_2 NPs, QDs can also be encapsulated inside polymer particles and later be spun to obtain fluorescent NFs. QDs are semiconductor nanocrystals with unique optical and electronic properties. They are well-known due to their size tuneable fluorescence emission, broad absorption spectra, specific emission signal, and high photostability.[45,46] In this work, crosslinked PS/PMMA core/shell polymer particles bearing 0.42 wbm % of QDs were synthesized (L_QDs) following the work of De San Luis et al.[40,47] The encapsulation of QDs into polymer particles protects the QDs surface against damage, protects the environment from the QDs toxicity, and makes easier the manipulation of the material.[47] L_QDs were mixed with the blank latex (L_Blank) and blended with the PVA solution to form the electrospinning blend (B_QDs). Again, the polymer particles/PVA ratio was 62/38 wt.%/wt.% and the s.c. 17%. **Figure 4** shows the TEM micrograph of latex L_QDs, as well as the TEM and SEM micrographs of the obtained NFs. Figure 4(a) displays that QDs were successfully encapsulated inside the polymer particles. Figure 4(b) shows that bead-free and uniform fibers with an average diameter of 207 ± 33 nm were obtained. Furthermore, the TEM micrograph (Figure 4(c)) demonstrates that a good distribution of the QDs along the NFs was obtained (additional TEM images are shown in the Supporting Information).

Fluorescence emission spectra of the blend B_QDs, as well as one of the NFs were also measured (**Figure 5**). The initial B_QDs electrospinning dispersion (Figure 5(a)) and the final NFs had exactly the same emission peak, no shifting nor broadening/narrowing of the emission peak was observed after the electrospinning process. Additionally, Figure 5(b) shows that the longer the electrospinning time, the higher the emission intensity of the NFs material. The reason is that the higher the electrospinning time, the thicker the obtained NFs mat and therefore the higher the amount of QDs in the material and the higher the fluorescence emission intensity. Thus, by controlling the electrospinning time, the fluorescence emission intensity of the material can be easily controlled using the same initial polymer blend.

3.3. Nanofibers Containing Different Types of Nanoparticles

Our next step was to obtain hybrid NFs with more than one type of inorganic NPs; to this end, electrospinning dispersions containing L_QDs and L_CeO_2_5% were prepared. Both latexes were first mixed with the blank latex at different ratios and then blended with the PVA solution. In this way, two different electrospinning blends were obtained; B_QDs_CeO_2_1:1 and B_QDs_CeO_2_1:2 (see Table 3). In sample B_QDs_CeO_2_1:1 the weight ratio between the CeO_2 and the QDs was 1 to 1, whereas

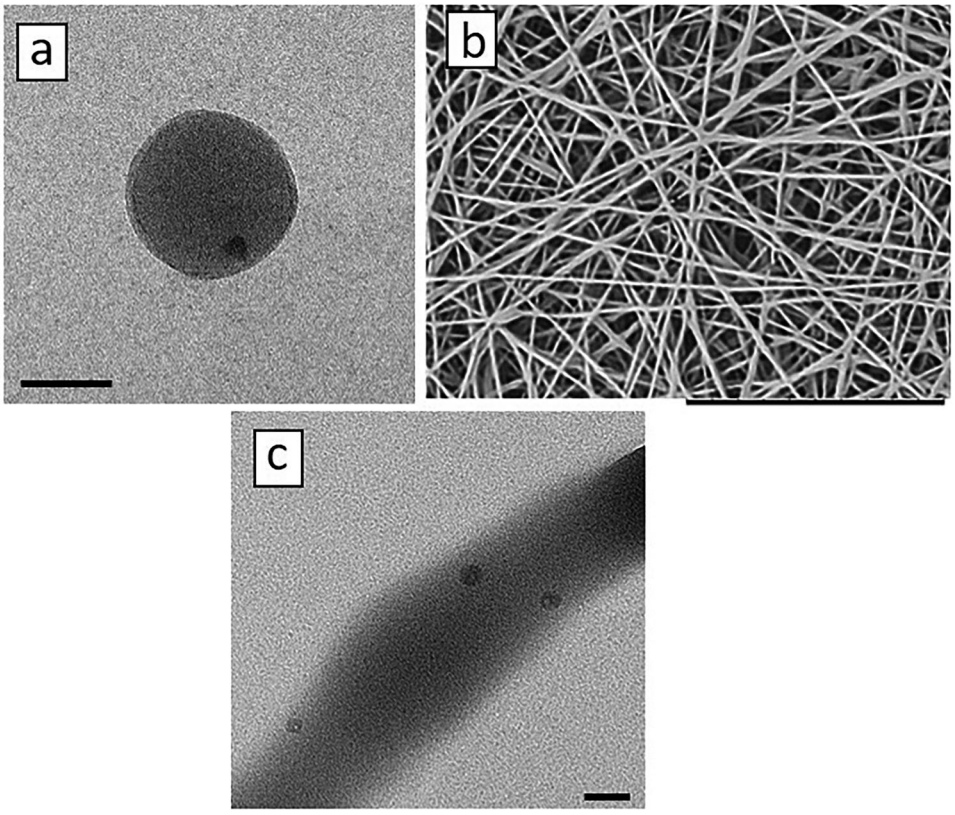

Figure 4. a) TEM micrograph of a polymer particle of latex L_QDs (scale bar: 50 µm) and SEM (b) and TEM (c) images of the NFs obtained from the blend B_QDs, respectively (scale bars: 50 nm and 10 µm respectively).

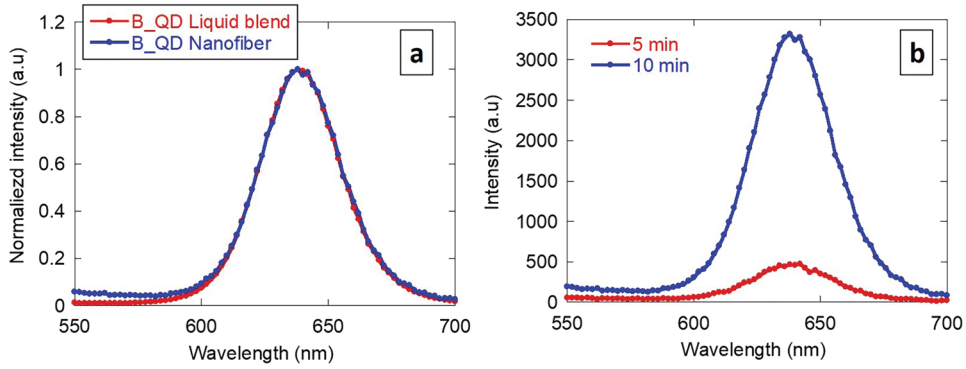

Figure 5. a) Fluorescence emission spectra of the initial electrospinning dispersion B_QDs and the obtained NFs. b) Fluorescence emission spectra of the NFs obtained from B_QDs collected for different periods of time.

in sample B_QDs_CeO_2_1:2 the weight ratio was 1 to 2. **Figure 6** and **Figure 7** show the SEM images, as well as the elemental maps of the NFs performed by XEDS in the STEM mode using a HAADF detector for the NP ratios 1:1 and 1:2, respectively.

Uniform NFs were obtained in both cases and the STEM images with XEDS mapping (Figure 6(c) and Figure 7(c)) demonstrate that the hybrid fibers contained two types of inorganic NPs: CeO_2 (marked in yellow) and QDs (marked in purple). The distribution of the inorganic NPs was very good in both cases without any aggregation. Additionally, by changing the ratio between latex L_QDs and L_CeO_2_5% in the initial dispersion, it was possible to change the ratio between CeO_2 NPs and the QDs in the final fibers.

Figure 8 shows that no significant differences were observed when measuring the average diameter of the NFs obtained from B_QDs, B_QDs_CeO_2_1:1, and B_QDs_CeO_2_1:2. Again, it is demonstrated that using green electrospinning, it is possible to obtain NFs with different types and concentrations of inorganic

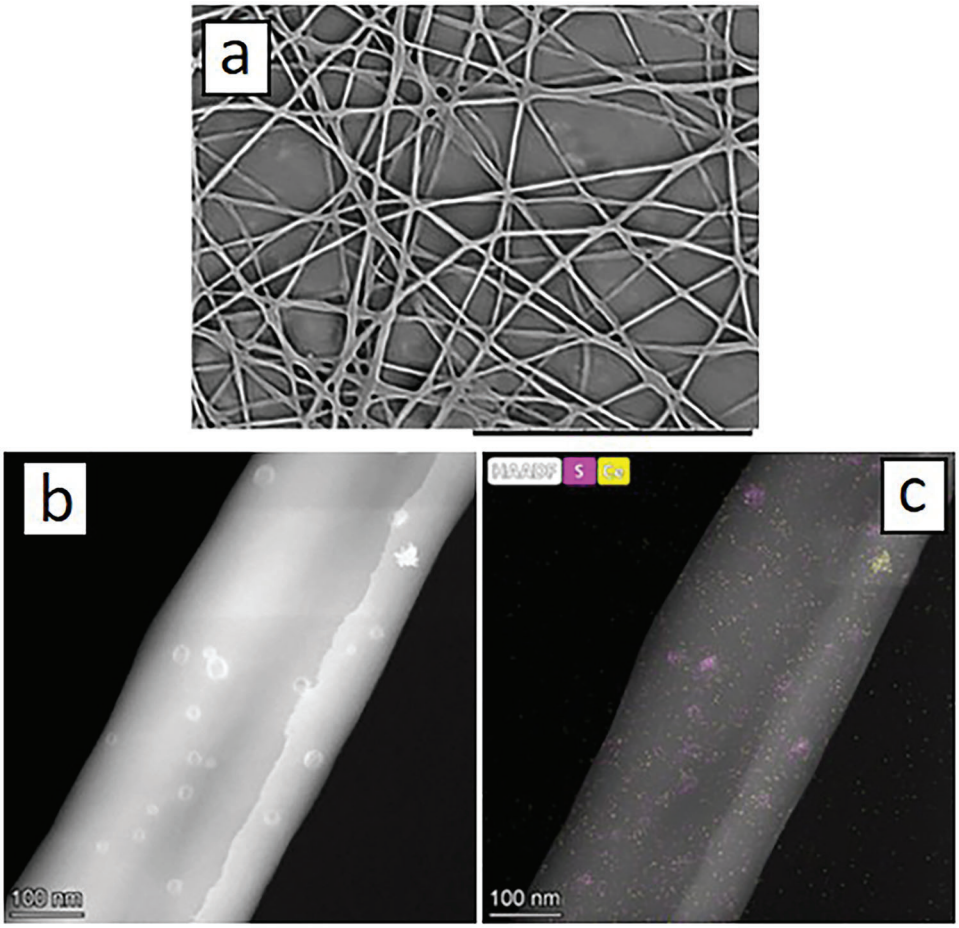

Figure 6. a) SEM (scale bar 10 µm), b) HAADF STEM and c) XEDS mapping images of the nanofibers obtained from the blend B_QDs_CeO_2_1:1. Yellow color of the XEDS mapping corresponds to Ce (in CeO_2 NPs) and purple to S (in QDs).

NPs, without suffering any aggregation and keeping constant the diameter of the fiber. As it has been explained before, this would not be possible to achieve using conventional solution electrospinning.

Fluorescent emission intensities of the electrospinning dispersions containing both types of inorganic NPs (B_QDs_CeO_2_1:1 and B_QDs_CeO_2_1:2), as well as of the ones of the obtained NFs were measured (**Figure 9**). All the samples were fluorescent, but the intensity of the fluorescence emission spectra decreased as the amount of CeO_2 NPs was increased. This phenomenon was observed in both cases, in the initial electrospinning blends and in the final NFs. We also measured the fluorescence emission of a mixture of QDs and CeO_2 NPs in toluene at different QDs:CeO_2 ratios and we also observed that the intensity decreased as the amount of the CeO_2 NPs was increased (results shown in section S.4 in the Supporting Information). We do not have any clear explanation for this phenomenon. De San Luis et al.[48] co-encapsulated QDs and CeO_2 NPs in the same polymer particles and formed films with the hybrid latexes. Interestingly they observed that the fluorescence emission intensity of both, the latex and the film, increased over time when the sample was exposed to sunlight. They claimed that the phenomenon was related to the antenna effect that CeO_2 NPs have upon receiving the incident optical radiation and transferring it to QDs enhancing their fluorescence. The hybrid NFs obtained in this work were also exposed to sunlight, but no significant increase of the florescence over time was observed. This might be due to the fact that in this work the QDs and CeO_2 NPs are located in different polymer particles and therefore they are not close enough to produce the antenna effect.

Up to now, we have demonstrated that using green electrospinning we can obtain NFs with two different types of inorganic NPs, but we could add as many inorganic NPs as desired and no aggregation in the final NFs would occur. As a proof of concept, electrospinning dispersion B_QDs_CeO_2_Fe_3O_4 was prepared by mixing L_QDs, L_CeO_2, and L_Fe_3O_4 (see Table 3). As can be observed in **Figure 10**, NFs with three different types of inorganic NPs were achieved: Fe_3O_4 (marked in red), QDs (marked in blue), and CeO_2 (marked in yellow). Thus, green electrospinning can be used to create multifunctional organic/inorganic hybrid NFs in a simple way, without using any organic solvent and controlling independently the NFs morphology and the amount and size of the inorganic NPs. QDs, CeO_2 NPs, and Fe_3O_4 NPs have been individually incorporated into NFs and claimed to form interesting materials for sensing[21,28,34] and biomedical applications.[22,49,50] In the present work, the three different inorganic NPs were

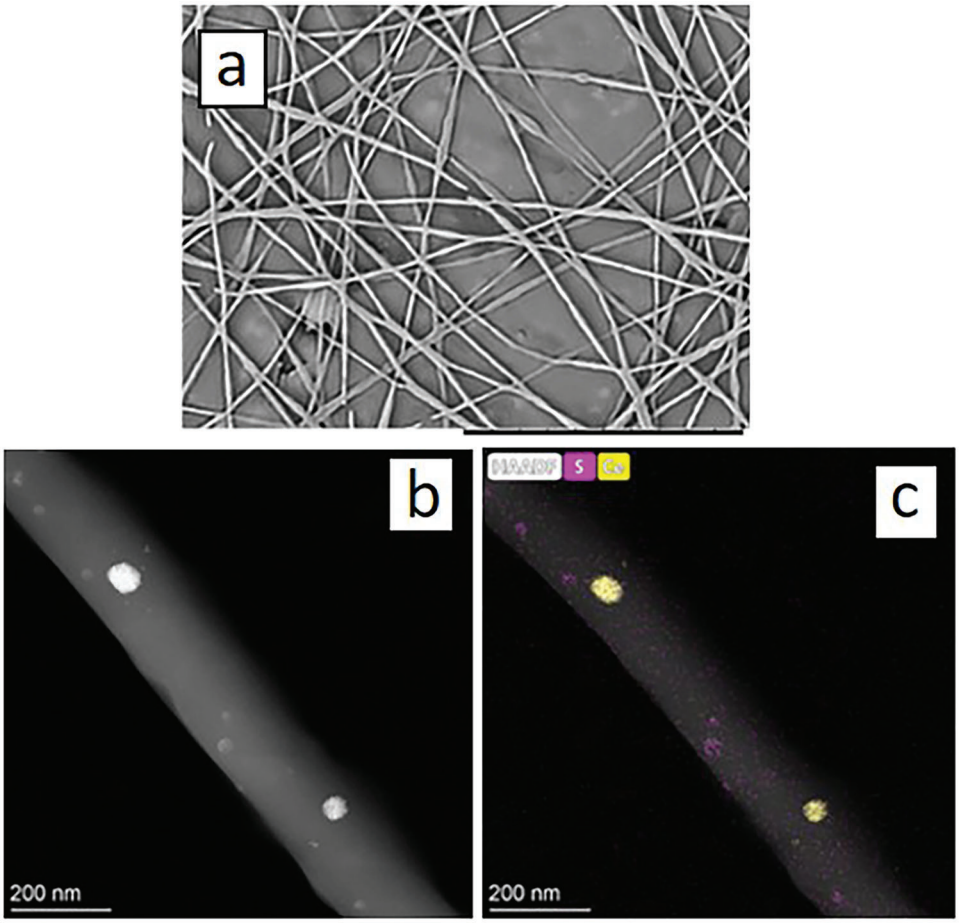

Figure 7. a) SEM, b) HAADF STEM, and c) XEDS mapping images of the nanofibers obtained from the blend B_QDs_CeO_2_1:2. Yellow color of the XEDS mapping corresponds to Ce and purple to S.

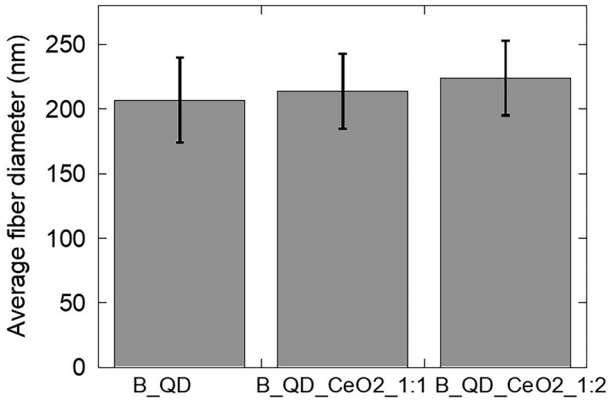

Figure 8. Average diameter of the NFs obtained from B_QDs, B_QDs_CeO_2_1:1 and B_QDs_CeO_2_1:2.

incorporated at the same time, therefore the obtained multifunctional material is also promising for those applications. The same technology could also be used to fabricate NFs containing fluorescent dyes, drugs, or other functional molecules.

4. Conclusions

In this work, green electrospinning has been used to create composite novel multifunctional nanofibers (NFs) bearing QDs, CeO_2 NPs, and Fe_3O_4 NPs. To this end, first, polymer particles containing the desired NPs have been synthesized by miniemulsion polymerization and then these latexes have been spun using PVA as template polymer. We have demonstrated that using green electrospinning it is possible to electrospun hydrophobic inorganic NPs using water as an electrospinning medium, fact that is not possible to achieve by conventional solution electrospinning. Not only that, a good distribution of the inorganic NPs along the fibers is achieved without any aggregation during the electrospinning process. Furthermore, by controlling the amount of the inorganic NPs that are encapsulated inside the polymer particles, it is possible to control the size of the inorganic NPs in the final NFs. Additionally, we have evidence that it is possible to change the concentration and size of the inorganic NPs without altering the NFs size, a fact that again it is not possible by conventional solution electrospinning. This allowed us to tune the properties of the composite NFs such as the fluorescence keeping the NF morphology intact. Finally, we have also proved that by using green electrospinning it is possible to obtain NFs with

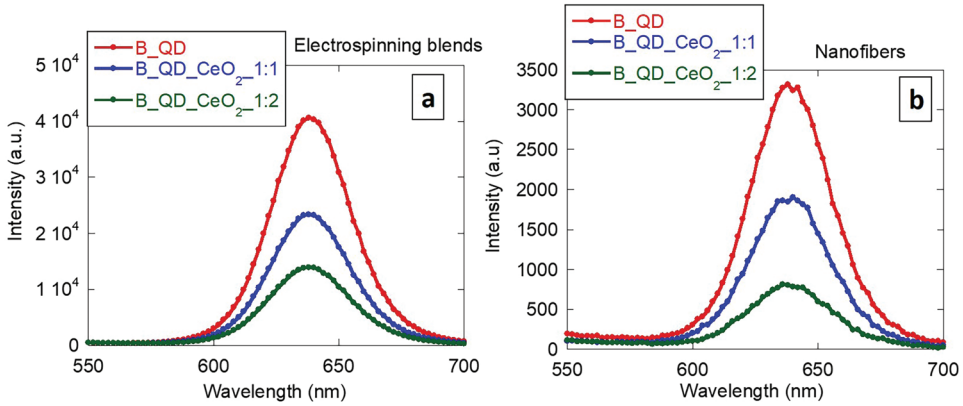

Figure 9. Fluorescence emission spectra of a) the initial electrospinning dispersions and the final NFs b) collected for 10 min.

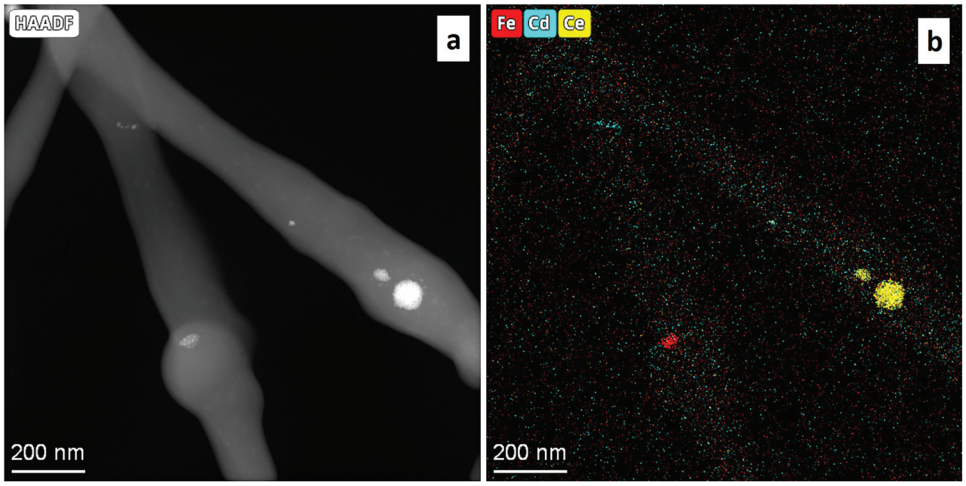

Figure 10. a) STEM and b) HAADF XEDS mapping images of the nanofibers obtained from the blend B_QDs_CeO_2_Fe_3O_4. Yellow color of the XEDS mapping corresponds to Ce, blue to Cd, and red to Fe.

different types of inorganic NPs (and therefore multiple functionalities) guaranteeing a good distribution and encapsulation with no aggregation of the NPs. This paper demonstrates that green electrospinning is a powerful and attractive technology to create novel composite (multi)functional NFs without the use of any organic solvent and opens the path to the development of any future application that might require them.

Supporting Information

Supporting Information is available from the Wiley Online Library or from the author.

Acknowledgements

The authors thank the technical and human support provided by SGIker (UPV/EHU/ ERDF, EU). The financial support from the Ministerio de Ciencia e Innovación (PID2020-117628RJ-I00 and PID2021-123146OB-I00) and the Basque Government (IT-1525-22) is gratefully acknowledged.

Conflict of Interest

The authors declare no conflict of interest.

Author Contributions

The manuscript was written with the contributions of all authors. All authors have given approval for the final version of the manuscript.

Data Availability Statement

The data that support the findings of this study are available in the supplementary material of this article.

Keywords

cerium oxide, electrospinning, functional nanofibers, green electrospinning, hybrid nanofibers, latex, quantum dots

Received: January 12, 2023
Published online: February 20, 2023

[1] J. Xue, J. Xie, W. Liu, Y. Xia, *Acc. Chem. Res.* **2017**, *50*, 1976.
[2] J. Xue, T. Wu, Y. Dai, Y. Xia, *Chem. Rev.* **2019**, *119*, 5298.

[3] M. Toriello, M. Afsari, H. K. Shon, L. D. Tijing, *Membranes* **2020**, *10*, 204.
[4] J. Yin, F. Zhan, T. Jiao, H. Deng, G. Zou, Z. Bai, Q. Zhang, Q. Peng, *Chin. Chem. Lett.* **2020**, *31*, 992.
[5] L. Zhang, K. Wei, J. Ma, J. Wang, Z. Liu, R. Xing, T. Jiao, *Appl. Surf. Sci.* **2021**, *566*, 150754.
[6] S. Agarwal, A. Greiner, *Polym. Adv. Technol.* **2011**, *22*, 372.
[7] D. Crespy, K. Friedemann, A.-M. Popa, *Macromol. Rapid Commun.* **2012**, *33*, 1978.
[8] E. Gonzalez, A. Barquero, B. Muñoz-Sanchez, M. Paulis, J. R. Leiza, *Nanomaterials* **2021**, *11*, 706.
[9] A. Stoiljkovic, M. Ishaque, U. Justus, L. Hamel, E. Klimov, W. Heckmann, B. Eckhardt, J. H. Wendorff, A. Greiner, *Polymer* **2007**, *48*, 3974.
[10] W. Yuan, K.-Q. Zhang, *Langmuir* **2012**, *28*, 15418.
[11] D. Cao, X. Li, L. Yang, D. Yan, Y. Shi, Z. Fu, *J. Appl. Polym. Sci.* **2018**, *135*, 46288.
[12] L. Buruaga, H. Sardon, L. Irusta, A. González, M. J. Fernández-Berridi, J. J. Iruin, *J. Appl. Polym. Sci.* **2010**, *115*, 1176.
[13] A. Stoiljkovic, R. Venkatesh, E. Klimov, V. Raman, J. H. Wendorff, A. Greiner, *Macromolecules* **2009**, *42*, 6147.
[14] E. Giebel, C. Mattheis, S. Agarwal, A. Greiner, *Adv. Funct. Mater.* **2013**, *23*, 3156.
[15] E. Klimov, V. Raman, R. Venkatesh, W. Heckmann, R. Stark, *Macromolecules* **2010**, *43*, 6152.
[16] E. Giebel, A. Greiner, *Macromol. Mater. Eng.* **2012**, *297*, 532.
[17] W. Huang, Y. Xiao, X. Shi, *Adv. Fiber Mater.* **2019**, *1*, 32.
[18] J. Yang, K. Wang, D.-G. Yu, Y. Yang, S. W. A. Bligh, G. R. Williams, *Mater. Sci. Eng.: C* **2020**, *111*, 110805.
[19] R. Sridhar, S. Sundarrajan, J. R. Venugopal, R. Ravichandran, S. Ramakrishna, *J. Biomater. Sci., Polym. Ed.* **2013**, *24*, 365.
[20] S. Agarwal, A. Greiner, J. H. Wendorff, *Prog. Polym. Sci.* **2013**, *38*, 963.
[21] I. A. A. Terra, L. A. Mercante, R. S. Andre, D. S. Correa, *Biosensors* **2017**, *7*, 61.
[22] C. J. Mortimer, C. J. Wright, *Biotechnol. J.* **2017**, *12*, 1600693.
[23] M. Li, J. Zhang, H. Zhang, Y. Liu, C. Wang, X. Xu, Y. Tang, B. Yang, *Adv. Funct. Mater.* **2007**, *17*, 3650.
[24] E. Atabey, S. Wei, X. Zhang, H. Gu, X. Yan, Y. Huang, L. Shao, Q. He, J. Zhu, L. Sun, A. S. Kucknoor, A. Wang, Z. Guo, *J. Compos. Mater.* **2013**, *47*, 3175.
[25] T. P. Mthethwa, M. J. Moloto, A. De Vries, K. P. Matabola, *Mater. Res. Bull.* **2011**, *46*, 569.
[26] X. Nie, S. Wu, A. Mensah, K. Lu, Q. Wei, *Mater. Sci. Eng.: C.* **2020**, *108*, 110377.
[27] N. Shehata, S. Gaballah, E. Samir, A. Hamed, M. Saad, *Nanomaterials* **2016**, *6*, 102.
[28] N. Shehata, E. Samir, S. Gaballah, A. Hamed, A. Elrasheedy, *Sensors* **2016**, *16*, 1371.
[29] W.-W. Dai, H.-F. Guo, D.-H. Qian, Z.-X. Qin, Y. Lei, X.-Y. Hou, C. Wen, *J. Mater. Chem. B* **2017**, *5*, 1053.
[30] R. Augustine, A. Hasan, N. K. Patan, Y. B. Dalvi, R. Varghese, A. Antony, R. N. Unni, N. Sandhyarani, A.-E. Al Moustafa, *ACS Biomater. Sci. Eng.* **2020**, *6*, 58.
[31] J. Saremi, M. Khanmohammadi, M. Azami, J. Ai, A. Yousefi-Ahmadipour, S. Ebrahimi-Barough, *J. Biomed. Mater. Res., Part A* **2021**, *109*, 1588.
[32] R. Tatavarty, E. T. Hwang, J.-W. Park, J.-H. Kwak, J.- O. Lee, M. B. Gu, *React. Funct. Polym.* **2011**, *71*, 104.
[33] S. B. Balakrishnan, S. Thambusamy, *Mater Today Commun* **2019**, *21*, 100664.
[34] T. Yang, P. Hou, L. L. Zheng, L. Zhan, P. F. Gao, Y. F. Li, C. Z. Huang, *Nanoscale* **2017**, *9*, 17020.
[35] C. Li, S. Shu, R. Chen, B. Chen, W. Dong, *J. Appl. Polym. Sci.* **2013**, *130*, 1524.
[36] M. Breitwieser, C. Klose, A. Hartmann, A. Büchler, M. Klingele, S. Vierrath, R. Zengerle, S. Thiele, *Adv. Energy Mater.* **2017**, *7*, 1602100.
[37] A. Jain, M. Behera, C. Mahapatra, N. R. Sundaresan, K. Chatterjee, *Mater. Sci. Eng.: C.* **2021**, *118*, 111416.
[38] S.-L. Quan, H.-S. Lee, E.-H. Lee, K.-D. Park, S. G. Lee, I.-J. Chin, *Microelectron. Eng.* **2010**, *87*, 1308.
[39] P. Philip, T. Jose, I. V. Vanchippurackal, *J. Appl. Polym. Sci.* **2021**, *138*, 50534.
[40] A. De San Luis, Z. Aguirreurreta, L. M. Pardo, A. Perez-Marquez, J. Maudes, N. Murillo, M. Paulis, J. R. Leiza, *Isr. J. Chem.* **2018**, *58*, 1347.
[41] M. Aguirre, M. Paulis, J. R. Leiza, *J. Mater. Chem.* **2013**, *1*, 3155.
[42] M. Aguirre, M. Paulis, J. R. Leiza, T. Guraya, M. Iturrondobeitia, A. Okariz, J. Ibarretxe, *Macromol. Chem. Phys.* **2013**, *214*, 2157.
[43] M. Naseri-Nosar, S. Farzamfar, H. Sahrapeyma, S. Ghorbani, F. Bastami, A. Vaez, M. Salehi, *Mater. Sci. Eng.: C.* **2017**, *81*, 366.
[44] X. Zhang, X. Chen, *Int J Polym Sci* **2019**, 2494586.
[45] C. J. Murphy, *Anal. Chem.* **2002**, *74*, 520A.
[46] N. Tomczak, R. Liu, J. G. Vancso, *Nanoscale* **2013**, *5*, 12018.
[47] A. De San Luis, A. Bonnefond, M. Barrado, T. Guraya, M. Iturrondobeitia, A. Okariz, M. Paulis, J. R. Leiza, *Chem. Eng. J.* **2017**, *313*, 261.
[48] A. De San Luis, M. Paulis, J. R. Leiza, *Soft Matter* **2017**, *13*, 8039.
[49] S. Wei, J. Sampathi, Z. Guo, N. Anumandla, D. Rutman, A. Kucknoor, L. James, A. Wang, *Polymer* **2011**, *52*, 5817.
[50] S. Ren, Y. Zhou, K. Zheng, X. Xu, J. Yang, X. Wang, L. Miao, H. Wei, Y. Xu, *Bioact Mater* **2022**, *7*, 242.

